INSTITUTE OF PLASMA PHYSICS

NAGOYA UNIVERSITY

RESEARCH REPORT

NAGOYA, JAPAN

Observation of Stationary Shock-like Structure and Enhanced Diffusion in a Toroidal Plasma

A. Mohri and M. Fujiwara

IPPJ-179 November 1973

Further communication about this report is to be sent to the Research Information Center, Institute of Plasma Physics, Nagoya University, Nagoya, Japan.

Synopsis

Electrons are injected into an afterglow plasma confined in a $\ell = 3$ stellarator to raise the poloidal rotational velocity. A steady shock-like structure characterized by a steep density gradient is observed near a critical rotational speed. A strong enhancement of diffusion rate occurs at higher radial electric field, accompanying with large amplitude density fluctuations. Vortices are generated at three corners of the triangular magnetic surfaces when the radial electric field turns over as going to the periphery.

1. INTRODUCTION

Problems of plasma rotation about the minor axis in toroidal systems have acquired much interest since the plasma diffusion rate is modified by introducing both density and potential variations over magnetic surfaces. Stringer[1] first found that the plasma is unstable against the poloidal rotation and the diffusion rate becomes infinite at a critical rotational speed $v_c \equiv (\varepsilon \iota/2\pi)c_s$ (here ι is the rotational transform, ε the inverse aspect ratio, and c_s the sound speed). Rosenbluth and Taylor[2], and Stringer[3] found that viscosity eliminates this singularity. Then, the presence of a stationary weak shock in equilibrium has been criticized by Hazeltine et al[4], Taniuti[5], Asano et al[6] and Green et al[7]. From computer simulations, Winsor et al[8], Bower et al[9], and Green et al[7] demonstrated the time evolution of the rotation and the shock structure in density and electrostatic potential. However, there has been no clear experimental evidence of these theoretical predictions. In case of plasma heating by a neutral beam injection, the radial electric field is possibly developed since some part of dissolved ions of the beam (banana particles) escape from the trapping region of plasma [10].

In this paper is described an experiment of the electron injection by a tiny emissive probe into the confined plasma in a $\ell = 3$ stellarator. By this injection it is possible to deliberately increase the radial electric field

until it reaches a sufficient value at which the rotation affects the plasma behaviour. Convective motions, which were observed just after the plasma production,[11), 12), 13)] can deliberately be formed, and shock-like structures in plasma density are observed as well as the strong enhancement of diffusion rate. This experiment could be regarded as a simulation of the neutral beam injection, under which the plasma is effectively supplied with excess electrons.

2. EXPERIMENTAL METHOD AND CONDITION

The experiment is made with JIPP-stellarator which is a circular $\ell = 3$ stellarator with the major radius of 50 cm with eight field periods. Helical coils of 10.4 cm minor radius are wound on the vacuum vessel of stainless steel whose inner radius is 8.4 cm. The stationary (5 sec) toroidal field B_t is 4 kG at maximum. The rotational transform ι is up to 1.7 π, and the shear parameter is up to 0.15. The well depth is variable from -5 % to 10 % by changing the vertical field. The field parameters in this experiment are $B_t = 875$ G, $\iota = 1.7\ \pi$ at the outmost magnetic surface with a mean radius of 3.4 cm, and the vertical field is not applied. Xenon plasma is produced by ECRH at 2.45 GHz. A microwave power of about 300 W is fed through

a coaxial cable and a loop antenna during 10 ms. The neutral gas pressure is 1.8×10^{-5} torr. The choice of xenon as the working gas comes from the reason that the sound velocity $(T_e/m_i)^{1/2}$, where T_e is the electron temperature and m_i the ion mass, is slow and the dielectric constant is fairly high even at the low density of plasma. The convective cells arising at the production stage damp faster in xenon plasma than the case of lighter ion plasmas[13]. Thus, it becomes easier to observe the change of the plasma structure when the emissive probe is used to inject electrons.

The plasma density is measured with a single Langmuir probe. The electron temperature T_e is inferred from both the characteristic curve of a pulse-scanning Langmuir probe and the phase velocity of ion acoustic waves which are externally excited. The electron temperature is 1.5 eV just after the ECRH, and it decreases to 0.6 eV during 10 ms. Then, the temperature becomes constant with time and its spatial variation is not observed except near the plasma periphery of 3 mm thick. For the measurement of the electrostatic field in the plasma, it would be favourable to use a hot emissive probe. However, the confinement time of density falls to about one-half when the emissive probe for the electron injection is inserted on the magnetic axis. The use of another emissive probe for the measurement would again cause more decrease of the confinement time. From this reason, the electrostatic field is also measured with a single Langmuir probe since the electron temperature is

constant most over the plasma region. The convective cells observed immediately after the ECRH damp with the time constant of 0.1 ms. Electrons are injected by the emissive probe at 50 ms after the ECRH, whence the confinement time is 32 ms, T_e = 0.6 eV, n = 1 × 10^9 cm^{-3} and the sound speed estimated from $(T_e/m_i)^{1/2}$ is 6.6 × 10^4 $cm \cdot s^{-1}$. It should be noted that this plasma is fairly viscous owing to its low ion temperature which is nearly room temperature. The viscosity perpendicular to the magnetic field can not be neglected because of the large mass of xenon ions, the Larmor radius of which is about 0.3 cm. The radial distribution of the floating potential is nearly parabolic as seen in fig.3. Thus, the poloidal plasma motion is a rigid body rotation, and the radial electric field is positive toward the plasma periphery and the potential on the axis is positive 30 ∿ 60 mV against the edge, which is nearly the same as the ion temperature 0.03 ∿ 0.05 eV.

A tiny hot emissive probe with a filament of barium-oxide coated tungsten is immersed inside the plasma, the position of which is on the magnetic axis, as shown in fig.1. The probe is negatively biased against the vaccuum vessel by an externally imposed pulse. The probe is always electrically isolated from the external pulse circuit, except the time of the pulse imposition. The isolation is mainly acertained by a zener-diode for very high frequency, the capacitance through which is only 3 pF. Therefore, the emissive probe is normally floating in the plasma so long

as the floating potential of the probe is positive to the wall. The electron current of the injection can be controlled by adjusting the negative pulse height on the emissive probe.

3. SPATIAL STRUCTURE OF PLASMA UNDER THE ELECTRON INJECTION

A rectangular negative pulse is applied on the emissive probe, the emitted electrons from which spread along the magnetic field. The front of the electron cloud propagates very fast, so that the resultant axial electric field vanishes in several microseconds.

(a) Case of moderate electron injection

A negative 3.5 V pulse is applied for 2.5 ms, when the injection current of electron becomes 24 μA. Figure 2 presents typical signals of the injection current, the floating potential and the ion saturation current of the probe. The injection current is fairly constant during the pulse, while the floating potential and the ion saturation current vary in complicated ways with time. These time variations at other places have different forms, because equi-potential and equi-density surfaces deform with time. The floating potential in the central region becomes deeply negative as the electrons are injected. In the outer region,

however, the potential remains still positive. Figure 3 shows this radial distribution. Thus, the electric drifts in the central and the outer regions become inverse with each other, and a large velocity shear appears at the interface of these regions. We can expect the occurrence of vortices at the interface, since the perpendicular viscosity is large in this case.

The time evolution of vortices can be followed with the spatial distributions of the electric potential and the density, as shown in fig.4. At 1 ms after the initiation of the electron injection, there appear three vortices at the corners of the triangular magnetic surface. These vortices exist for about 1.5 ms. Then, they go to rotate azimuthally and the clear pattern of the vortex fades out. The time variation of the potential is in agreement with the estimation from both the specific dielectric constant $\varepsilon_p \sim 3000$ and the number of injected electrons.

The origin of convective cells, which were observed just after the plasma formations such as ECRH and J × B gun,[11), 12), 13)] seems to be in the similar process. The radial distribution of the floating potential during the ECRH is shown in fig.5. There are also counter electric drifts, though the directions of the streams are inverse to those in case of the electron injection.

(b) Case of stronger injection

When the emissive current is sufficiently large, the resultant radial electric field becomes strong enough to

bring out its another effect. Figure 6 shows the time variations of structures in the case that the emissive current is about 100 μA and the pulse width is 1 ms. The other parameter are the same in the previous case. At the early stage (t = 0.1 ms in the figure), three vortices appear as previously shown in fig.4. They begin to rotate about the magnetic axis with large deformation in shape (t = 0.2 ∿ 0.3 ms). Then, two kinds of azimuthal density steepenings come out (t = 0.4 ∿ 1 ms): the one (A type) is near the middle radius on the inner side of the torus, and the other (B type) is found on the middle sides of triangles of the outer magnetic surfaces. The steepening of A type rapidly decreases after the end of the injection. Therefore, its origin is possibly due to the forced stress for the rotation by the electron injection. On the other hand, the steepenings of B type retain for 1 ms after the end of the injection. The radial distribution of the potential gradually varies to a nearly parabolic one (t = 1.8 ms), whence the azimuthal drift is likely a rigid body rotation.

The variation of the magnetic field over the cross section is large for $\ell = 3$ stellarator. We shall examine a critical velocity on the outer region where the effect of the helical field is dominant. The electron temperature T_e is 20 times the ion temperature, so that the fluid model is applicable to consider the presence of characteristic manifolds. Since the aspect ratio is so large as 20, we simplify the magnetic field to be a linear helical field

expressed by the scalar potential

$$B_0[Z + \frac{\varepsilon_h}{\alpha} I_\ell(\ell\rho)\sin\ell(\phi - \alpha z)] \qquad (1)$$

in cylindrical coordinates (r, ϕ, Z), where $\rho = \alpha r$, ℓ is the helical pole number and B_0 the external uniform field. We consider the case that a characteristic manifold lies on a helical line $\phi - \alpha Z = \text{const.}$ and that the electrostatic potential of plasma ϕ is constant on the magnetic surface ψ. Using a method similar to that employed by Taniuti and Asano[5), 6)] we get a critical rotational drift velocity for slow magnetosonic wave in low β case as

$$v_d^2 = \left|\frac{1}{B}\frac{\partial\Phi}{\partial\psi}\nabla\psi\right|^2 = c_s^2[(\frac{B}{B_0})^2(1 + \rho^2) - 1]. \qquad (2)$$

For small ρ and $\ell = 3$, the above equation is approximately written as

$$\frac{1}{C_s}\frac{\alpha\Phi_s}{B_0} = \pm\frac{\rho_{os}^2}{2}[1 - \varepsilon_h \frac{27}{16}\rho^3\cos3(\phi - \alpha Z)], \qquad (3)$$

where Φ_s is the potential difference between on the axis and on the separatrix whose average radius is ρ_{os}. The potential Φ has been assumed to be proportional to ρ_0^2, where ρ_0 is the average radius of a magnetic surface[14)]. This radial dependence of Φ corresponds to a rigid body rotation in a sense of average. Introducing the parameters of the plasma and the magnetic field, the potential dif-

ference given by eq.3 becomes 0.3 volt when the manifold is present at the position $\cos 3(\phi - \alpha Z) = -1$ on the outmost magnetic surface. In order to compare the experiment, we must further introduce the toroidicity even at the edge. In practice, there is not present the density steepening on the upper side of the triangular magnetic surface in fig.6. The estimated potential well agrees with the experimental one which is around -0.45 volt at t = 1.8 ms. The electron temperature in this stage is also measured by the pulse scanning probe and it does not changed from the initiation of the electron injection. The observed density steepening also resembles the result of the numerical analysis[7] in which the potential becomes positive. There is no clear calculation on the existence of stationary shock, which is useful to our case, but it is most possible that the observed azimuthal density steepening of B type is a stationary shock.

The minor axial variation of the structure is also measured. The position of the B type steepening is always observed near the side of outer triangular magnetic surfaces. Therefore, it is clear that this steepening originates in the non-circular cross section of the stellarator configuration.

4. ENHANCED DIFFUSION DUE TO RADIAL ELECTRIC FIELD

In this section, the effect of the radial electric field on the transport is described. The time duration of the electron injection is prolonged to 100 ms to observe the decay time of the plasma density. The radial electric field is changed by adjusting the negative pulse height on the emissive probe. When the emissive probe is floating in plasma, the confinement time is 32 ms at 50 ms after the turn off of ECRH.

The decay time of the plasma density is much related with the radial electric field. At high radial field, the decay time becomes very short as shown in fig.7. There are also observed large amplitude fluctuations in the density. The dependences of the decay time and the amplitude of the fluctuation on the radial electric field are shown in fig.8(a). The sharp decrease of the decay time and the strong growth of the amplitude are well correlated to each other. Figure 8(b) shows that the density fluctuation changes its frequency with the radial electric field. The poloidal wave mode number m is 1 and its frequency f nearly obeys the relation

$$f = (1 - \delta)E_r/(2\pi\bar{r}B_0) + \text{const.}$$

(experimentally $\delta \simeq 0.5$),

where E_r is the radial electric field, $\bar{r}$ the average minor radius of magnetic surface, B_0 the toroidal magnetic field and δ the correction parameter due to the Larmor radius effect of ions. Such a fluctuation is also observed in the early time after the turn off of ECRH[15]. This instability is mainly caused by the difference of electric drift between ions and electrons[16]. Ions with large Larmor radius feel the spatial distribution of the radial electric field so that the drift velocity becomes somewhat slower than the electron drift velocity and the centrifugal force on ions also gives the same effect. The dispersion relations applicable to this experimental condition are derived by Dodo[16] and Terashima[17], including the perpendicular viscosity and the parallel electron-ion collision. The poloidal wave mode number m and the toroidal one n may have the relation

$$Rk_{//} = m\iota + n, \qquad (4)$$

where R is the major radius of the torus, $k_{//}$ the parallel wave number and ι (= $\iota/2\pi$) the rotational transform. Therefore, $k_{//}$ varies widely in this case because ι is proportional to $\bar{r}^2$ in ℓ = 3 stellarator. Numerical results on the dispersion relation of ref.16 indicate there is fairly strong dependence of the frequency on both the ion temperature and $k_{//}$. In fig.8(b) is presented a numerical result of the frequency where the used plasma parameters are T_i = 0.03 eV, T_e = 0.6 eV, $k_{//} = 3 \times 10^{-4}$ cm^{-1} and δ = 0.45. The

observed frequency variation with the radial electric field qualitatively well agrees with the numerical result. Here the parameter δ depends on the ion Larmor radius ρ_i and the characteristic length of the radial electric field inhomogeneity Λ, according to the relation

$$\delta \simeq 1 - \exp\{-\pi^2 \rho_i^2/\Lambda^2\}.$$

The case $\delta = 0.45$ corresponds to $\rho_i = 0.3$ cm ($T_i = 0.03$ eV) and $\Lambda \simeq 1$ cm. This ion temperature is only an estimation from the collisional cooling of ions with the residual gas atoms. Also, large radial variation of the rotational transform makes the problem complicated. However, it is very possible that this observed fluctuation comes from above instability, because, theoretically and experimentally, the frequency deviation from $E_r/(2\pi\bar{r}B_0) \equiv f_d$ is on the lower side of f_d and nearly proportional to f_d.

5. CONCLUSIVE REMARKS

In order to study the influence of the minor-radial electric field on plasma behaviours in toroidal systems, electrons are deliverately injected into the afterglow plasma in JIPP-stellarator. The xenon plasma produced by ECRH is used in the experiment. The electric potential on the axis is positive 0.03 $\sim$ 0.05 V, and T_e is 0.6 eV. The electric drift velocity is in the direction of the ion diamagnetic velocity and the associated potential difference between on the axis and at the periphery is nearly equal to the ion temperature. When electrons are injected by the small emissive probe set on the axis, vortices are first formed at the three corners of the triangular magnetic surface, and then stationary shock-like structure appears on the sides of the triangle. The vortices only exist during the transient stage where the direction of the electric drift turns over inside the plasma. The observed vortices just after the plasma formations, such as ECRH and J × B gun, are possibly due to the same reason or the appearence of vortex at the interface between counter streams. The azimuthal density steepening occurs at the rotational speed near the critical velocity which is derived for $\ell = 3$ magnetic field. It should be noted that this density steepening is stationary in the experimental frame for 1.0 ms. A strong enhancement of the diffusion rate can be observed, and it is possibly due to the instability arising from the

difference of electric drift velocity between ions and electrons. It should be emphasized that the injected electron current of 20 $\sim$ 200 μA is enough to draw out the above mentioned phenomena. If a part of energetic ions of injected neutral beam escape from the containment region, then the plasma would be affected by the resultant excess electrons as in this experiment. The magnetic field of $\ell = 3$ stellarator largely changes its parameters such as the magnetic shear and rotational transform over the cross section. Therefore, similar experiment in $\ell = 2$ stellarator is now under preparation in order to have more clear comparison with theory.

ACKNOWLEDGEMENT

The authors would like to express their sincere gratitude to Prof. K. Matsuura for the suggestion of use of the emissive probe. The author also wish to thank Dr. T. Dodo for kind discussions on the instability and offering his numerical results. Thanks also due to Prof. Y. Terashima for discussion on the instability and to Prof. K. Miyamoto for continuous encouragement. They are deeply indebted to Prof. T. Taniuti for helpful discussion on the shock condition.

References

1) STRINGER, T. E., Phys. Rev. Letters 22 (1969) 770.

2) ROSENBLUTH, M. N., TAYLOR, J. B., Phys. Rev. Letters 23 (1969) 367.

3) STRINGER, T. E., Phys. Fluids 13 (1970) 1586.

4) HAZELTINE, R. D., LEE, E. P., ROSENBLUTH, M. N., Phys. Fluids 14 (1971) 361.

5) TANIUTI, T., Phys. Rev. Letters 25 (1971) 1478.

6) ASANO, N., TANIUTI, T., Phys. Fluids 15 (1972) 423.

7) GREENE, J. M., WINSOR, N. K., Princeton Plasma Phys. Lab. Report MATT-908 (1972).

8) WINSOR, N. K., JOHNSON, J. L., DAWSON, J. M., J. Comp. Phys. 6 (1970) 430.

9) BOWERS, E., WINSOR, N. K., Phys. Fluids 14 (1971) 2203.

10) STIX, T. H., Plasma Phys. 14 (1972) 367.

11) MIYAMOTO, K., MOHRI, A., INOUE, N., FUJIWARA, M., YATSU, K., TERASHIMA, Y., ITATANI, R., in Plasma Physics and Controlled Nuclear Fusion Research (Proc. 4th Int. Conf. Madison, 1971) 3, IAEA, Vienna (1971) 93.

12) MIYAMOTO, K., MOHRI, A., INOUE, N., FUJIWAKA, M., YATSU, K., Phys. Fluids 14 (1971) 2748.

13) FUJIWARA, M., MIYAMOTO, K., Nucl. Fusion 12 (1972) 587.

14) MOHRI, A., under contribution.

15) DODO, T., FUJIWARA, M., MIYAMOTO, K., OGATA, A., Proc. of Sixth European Conference on Controlled Fusion and Plasma Physics (Moscow, 1973) vol.I, p.121.

16) DODO, T., FUJIWARA, M., MIYAMOTO, K., OGATA, A., to be published in Proc. of Sixth European conference on Controlled Fusion and Plasma Physics (Moscow, 1973), vol.II.

17) TERASHIMA, Y., private communication, where the centrifugal force on ions due to the rotation is taken into account. The frequency shift from $mE_r/(2\pi\bar{r}B_0)$ as a function of E_r behaves as in ref.16.

Figure Captions

Fig.1. Schematic diagram of the electron injection circuit.

Fig.2. Oscillograms of the bias potential of the emissive probe V_b(5 V/div.), the emission current I_b(10 μA/div.), the floating potential detected by the Langmuir probe V_f(50 mV/div.) and the ion saturation current I_p(arb.unit). The time scales are 500 μs/div.. The bias potential is applied at 50 ms after the turn off of ECRH.

Fig.3. Radial distribution of the floating potential on the meridian plane of the torus. The solid line shows the case at 0.5 ms after the initiation of the electron injection, and the dotted line corresponds to the case just before the injection.

Fig.4. Spatial distributions of the equi-potential and the equi-density surfaces. The electron injection starts 50 ms after the turn off of ECRH. The injection current is about 20 μA. The direction of the toroidal field is downward the figure. The time noted is from the start of the injection. The numbers in the figures of the potential distributions are in millivolt.

Fig.5. Radial distribution of the floating potential V_f at 1 ms after switching on the ECRH microwave power.

Fig.6. Spatial distribution of the equi-potential and the equi-density surfaces. The electron injection

current is about 100 μA. The direction of the toroidal field is downward the figure. The time noted is from the start of the injection. The numbers in the figures of the potential distributions are in volt.

Fig.7. Time sweep of the ion saturation current I_p in the case of V_b = -6.0 V.
The upper trace: sweep rate is 10 ms/div.,
The lower trace: sweep rate is 2 ms/div..

Fig.8. (a) Dependences of the confinement time and the amplitude of the density fluctuation on the radial electric field E_r at r = 2 cm. The electron injection starts at 50 ms after the turn off of ECRH. The amplitude is measured at 12 ms after the initiation of the electron injection.

(b) Observed frequency as a function of E_r at r = 2 cm, and a theoretical curve dotted line of the frequency in the case T_i = 0.03 eV, T_e = 0.6 eV, δ = 0.45 and $k_{//} = 3 \times 10^{-4}$ cm^{-1}. $f_d = E_r/(2\pi\bar{r}B_0)$.

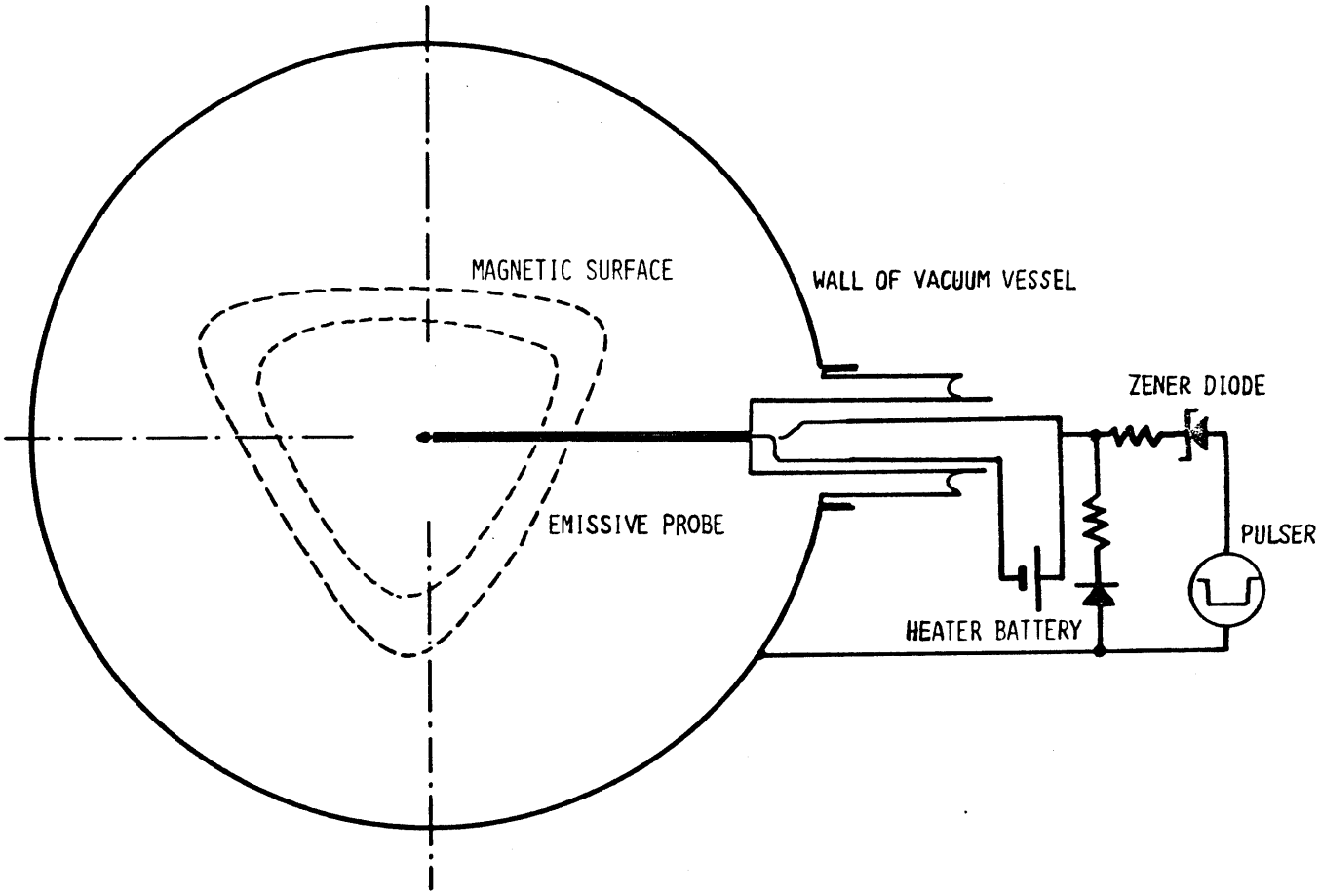
MAGNETIC SURFACE
WALL OF VACUUM VESSEL
ZENER DIODE
EMISSIVE PROBE
PULSER
HEATER BATTERY

FIG. 1

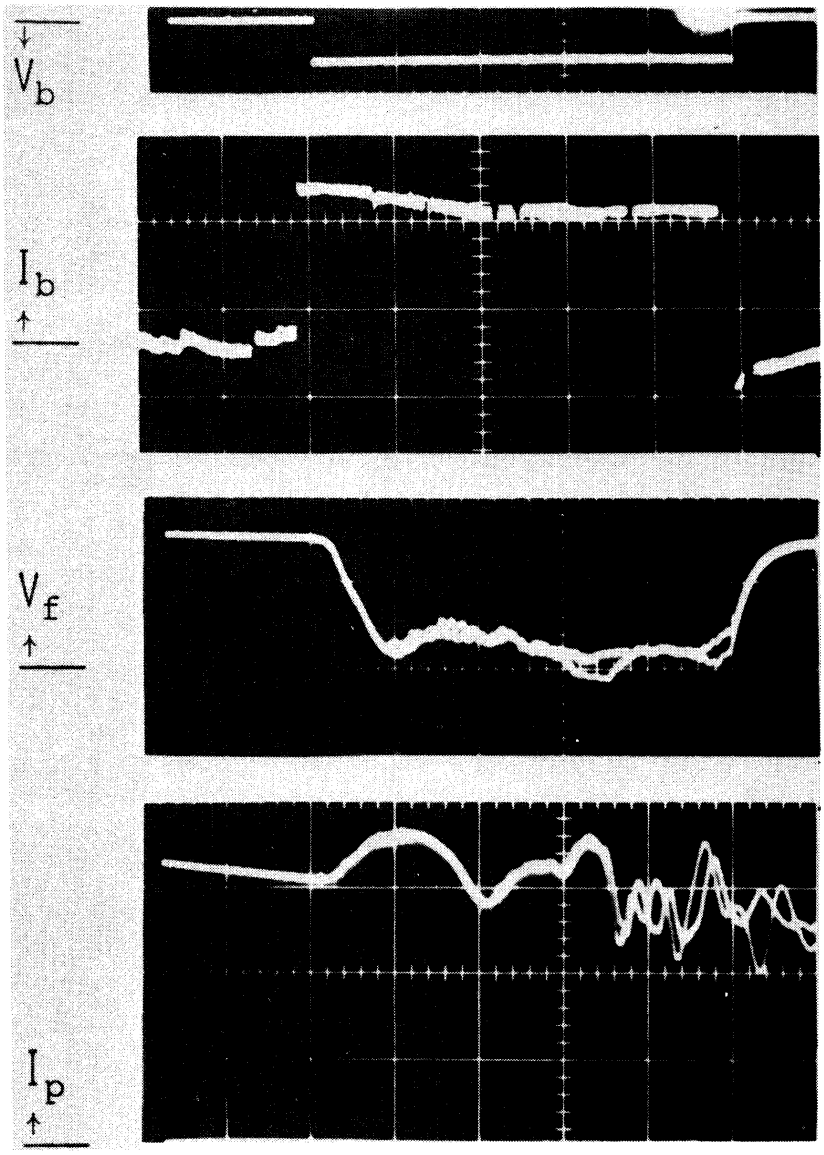

FIG.2

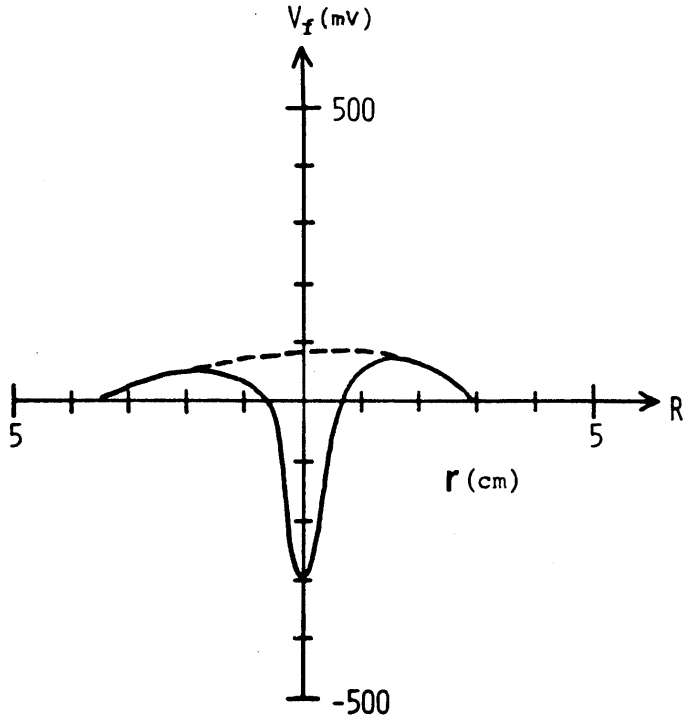

FIG. 3

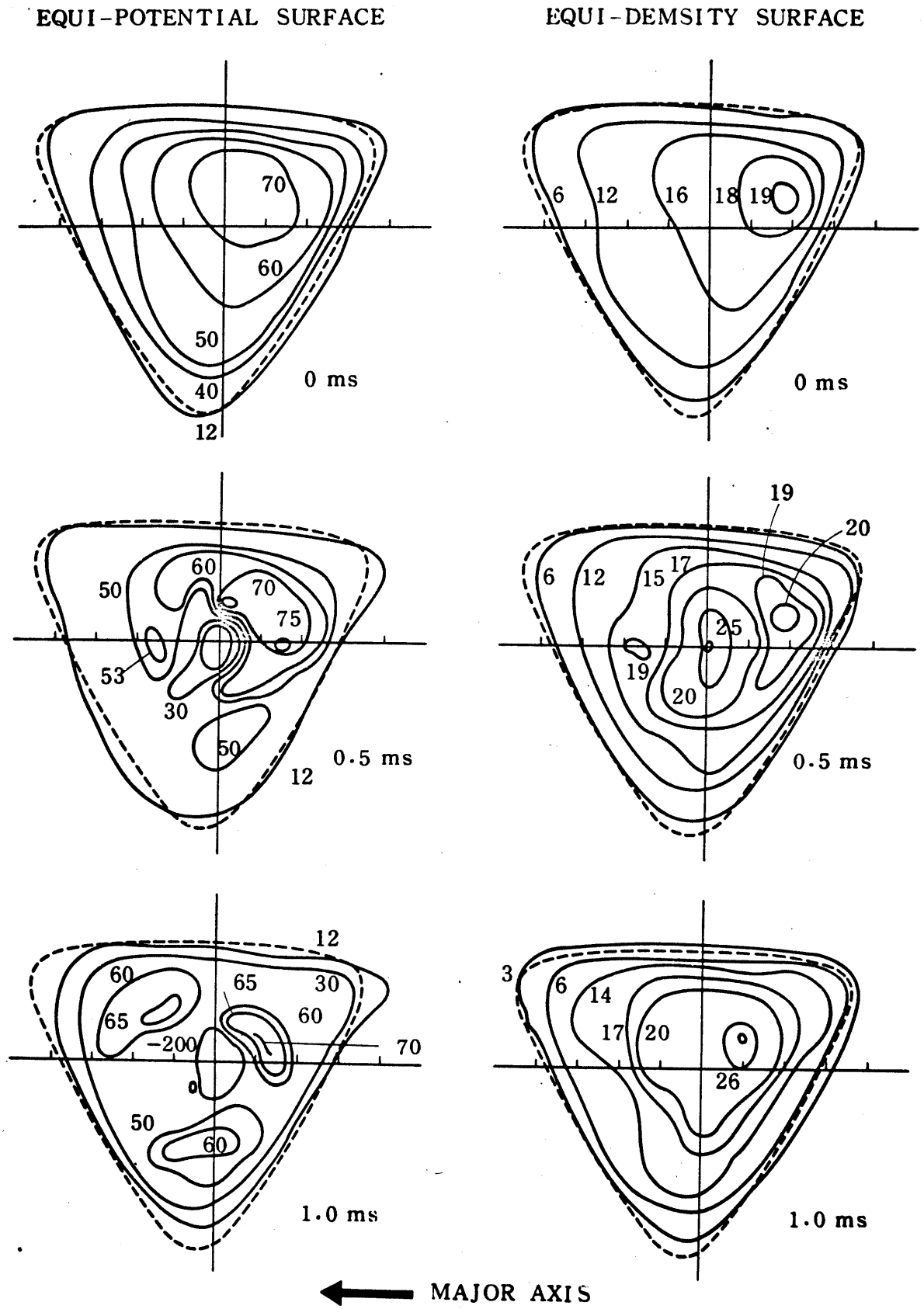
EQUI-POTENTIAL SURFACE
EQUI-DEMSITY SURFACE
70
60
50
40
12
0 ms
6
12
16
18
19
0 ms
60
50
70
75
53
30
50
12
0.5 ms
19
20
6
12
15
17
25
19
20
0.5 ms
12
60
65
30
65
60
-200
70
50
60
1.0 ms
3
6
14
17
20
26
1.0 ms
MAJOR AXIS

FIG. 4

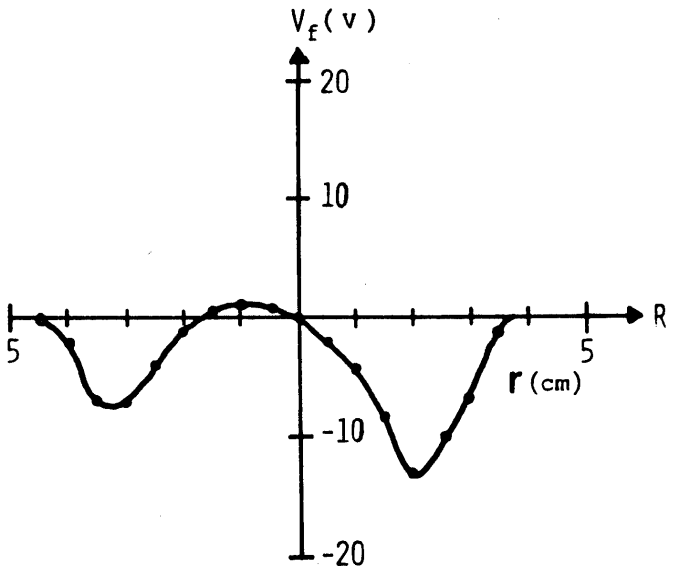

FIG. 5

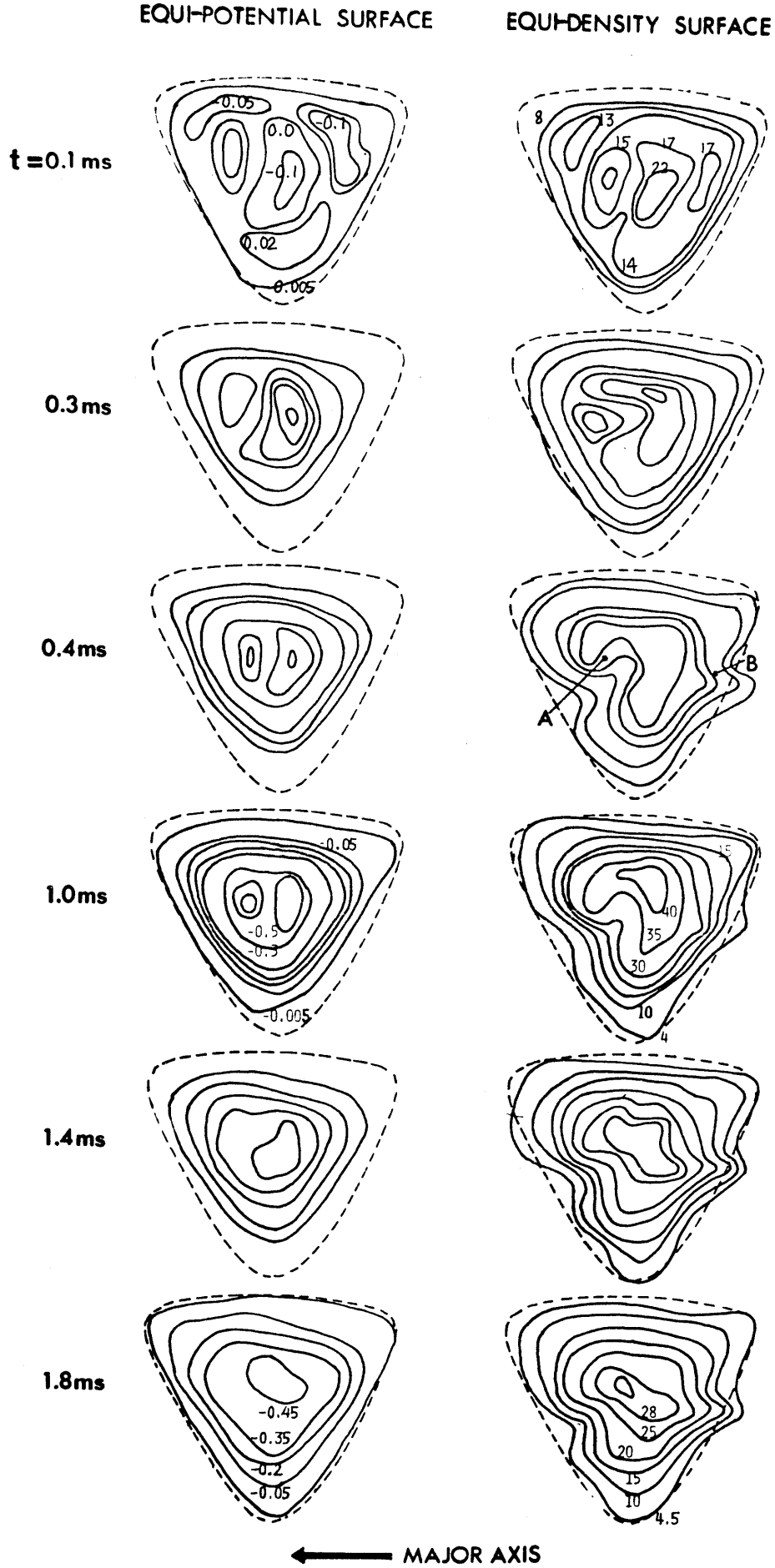
EQUI-POTENTIAL SURFACE
EQUI-DENSITY SURFACE
t = 0.1 ms
0.3 ms
0.4 ms
1.0 ms
1.4 ms
1.8 ms
-0.05
0.0
-0.1
-0.1
0.02
-0.005
8
13
15
17
17
22
14
A
B
-0.05
-0.5
-0.3
-0.005
40
35
30
10
4
-0.45
-0.35
-0.2
-0.05
28
25
20
15
10
4.5
MAJOR AXIS

FIG. 6

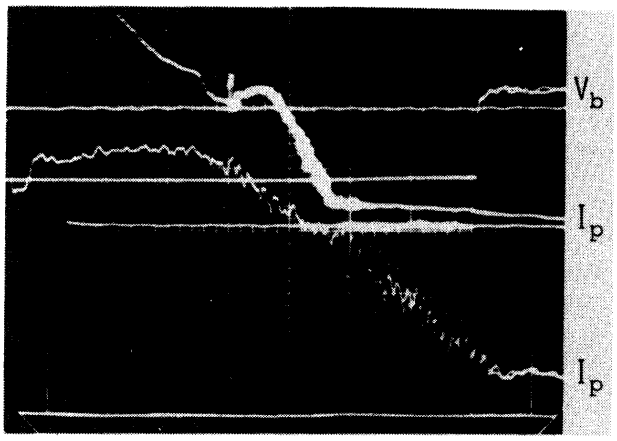

FIG.7

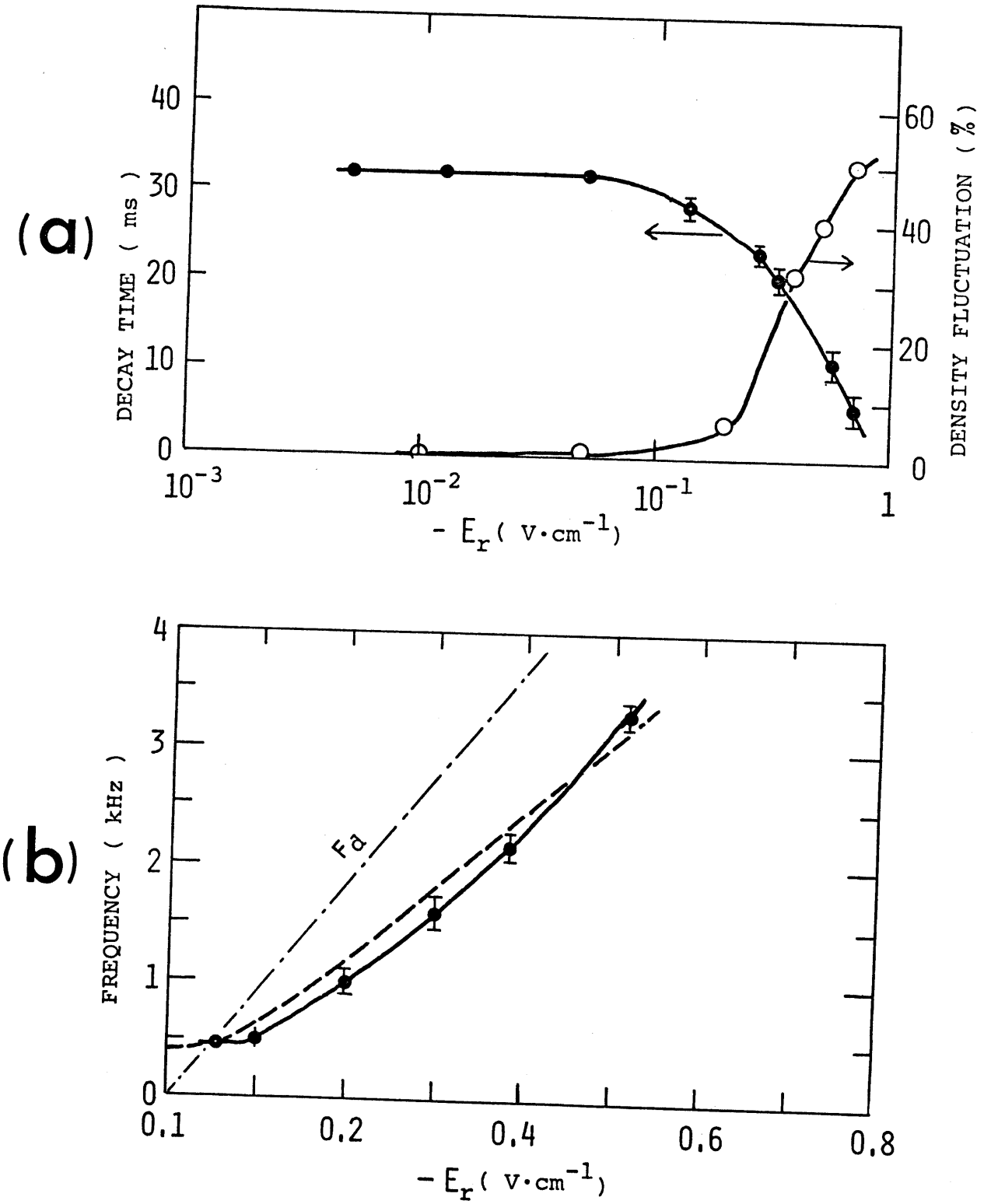
(a)
DECAY TIME (ms)
DENSITY FLUCTUATION (%)
40
30
20
10
0
60
40
20
0
10^{-3}
10^{-2}
10^{-1}
1
$-E_r$ ($v \cdot cm^{-1}$)
(b)
FREQUENCY (kHz)
4
3
2
1
0
Fd
0.1
0.2
0.4
0.6
0.8
$-E_r$ ($v \cdot cm^{-1}$)

FIG. 8